

Magnetic Resonance Elastography of the Heart

Thomas Elgeti · Ingolf Sack

Published online: 7 January 2014
© Springer Science+Business Media New York 2014

Abstract Cardiac magnetic resonance (MR) elastography noninvasively provides mechanics-based image contrast. The measurement of mechanical parameters is otherwise possible only by palpation or invasive pressure measurement. Measurement of parameters of myocardial shear stiffness is considered to be diagnostically beneficial especially in patients with diastolic dysfunction due to diffuse myocardial disease. Initial results of several single-center studies in animals, healthy volunteers, and patients suggest that cardiac MR elastography is capable of measuring shear stiffness-related diagnostic parameters. The following article shortly reviews the two main approaches used for cardiac MR elastography and outlines the results of the studies performed so far.

Keywords Cardiac MR elastography · Heart · Diastolic dysfunction · Myocardial shear modulus

Introduction

The pumping function of the heart relies on the periodic alteration in myocardial shear modulus.

Ventricular blood ejection, blood circulation, and pressure generation are maintained by the alteration in myocardial shear modulus—the driving force of our vascular system.

This article is part of the Topical Collection on *Molecular Imaging*

T. Elgeti (✉)
Klinik und Hochschulambulanz für Radiologie,
Charité - Universitätsmedizin Berlin, Campus Benjamin
Franklin, Hindenburgdamm 30, 12203 Berlin, Germany
e-mail: thomas.elgeti@charite.de

I. Sack
Institut für Radiologie, Charité - Universitätsmedizin Berlin, Campus
Mitte, Charitéplatz 1, 10117 Berlin, Germany
e-mail: ingolf.sack@charite.de

Magnetic resonance elastography (MRE) of the heart aims at measuring myocardial shear modulus in a noninvasive, image-resolved way. Therefore, cardiac MRE is a unique medical imaging modality that directly probes the source of cardiac function.

Cardiac failure is a considerable health burden and consumes a large share of medical resources. In the United States, more older persons are hospitalized for heart failure than for any other medical condition [1]. Its prevalence increases with age [2], and an estimated 5 million persons in the US and 23 million people worldwide [3] are considered to be affected. It is expected that, with increased aging of the population, the impact of heart failure will rise significantly [1]. To guide and monitor future therapy, proper diagnosis and follow-up of cardiac function are essential.

Traditionally, the diagnosis of cardiac failure has relied on the measurement of left ventricular ejection fraction (LV-EF). Using this approach, cardiac failure with preserved and reduced LV-EF is distinguished. The more severe the systolic dysfunction, the more the EF is reduced and, in general, the greater the end-diastolic and end-systolic volumes [4]. Medical imaging serves to mathematically calculate EF by dividing the stroke volume by end-diastolic volume [4]. While this approach is sufficient to diagnose systolic function, it is more difficult to assess diastolic function. It is known that, in more than half of cases, cardiac failure affects diastolic function [5].

In the past, measurement of volume–pressure–curves [6, 7] were considered the standard of reference for evaluation of diastolic function. Pressure changes in the cardiac chambers result from myocardial contraction and relaxation. Hence, pressure–time curves are directly related to the evolution of the myocardial shear modulus over the cardiac cycle. This measurement is an invasive procedure that is limited in daily clinical practice by the hazardous aortic valve passage in elderly patients [8]. Furthermore, the differentiation between intrinsic

myocardial changes and extrinsic factors (e.g., pericardium and right ventricle) can be challenging [7]. Therefore, echocardiography with tissue Doppler techniques serves as the standard of reference in clinical routine, supplemented by serological parameters (BNP, pro-NT-BNP) [4].

Cardiac MR imaging can visualize myocardial perfusion and the distribution of myocardial scar, enabling differentiation between ischemic and nonischemic cardiac disease [9, 10].

Nevertheless, noninvasive diagnosis of diffuse structural myocardial changes continues to be difficult, since distinct macroscopic features, as seen by conventional imaging techniques, have limited predictability. Cardiac MR imaging is considered the standard of reference for assessment of myocardial volumes and mass. Volume-time functions of the ventricle can therefore serve to assess not only systolic ejection fraction but also time-volume changes during diastole [11]. Recent technical advances have led to cardiac imaging techniques that allow performing breath-held measurement of transmitral flow [11]. Tagging is a further MR-based method which has been established for evaluation of the diastolic phase of the cardiac cycle [12]. All of these methods characterize myocardial tissue structure only indirectly and cannot quantify myocardial shear modulus. Quantification of elastic constants ultimately requires knowledge of both the stress field and strain distribution in the tissue under investigation. While measurement of strain is feasible by several of the aforementioned imaging modalities, cardiac stress can only be directly measured by invasive pressure probes mounted on catheters or by extrinsic activation using time-harmonic stress waves, which propagate through the thoracic wall into the heart and are utilized by MRE.

At this point, it should be mentioned that ultrasound-based cardiac elastography is an active area of research. Aspects of this technique that have been investigated include model assumptions about the elastic behavior of the myocardium [13], the measurement of the shock wave induced by aortic valve closure [14], and tissue activation by acoustic radiation forces or external oscillatory stress [15–17]. The principle of ultrasound elastography based on time-harmonic stress waves is similar to that of MRE and was derived by knowledge gathered in MRE [17].

Today, MRE is in clinical use for staging liver fibrosis. The results of pilot studies indicate that MRE allows differentiation between benign and malignant lesions in the breast, liver, and prostate [18–20]. Furthermore, MRE of the brain has shown to be sensitive in detecting early changes in multiple sclerosis [21]. In the heart, it is expected that MRE can improve the diagnosis of early forms of diffuse structural changes of the myocardium causing diastolic dysfunction and relaxation abnormalities [22, 23]. Several recent studies have shown that cardiac MRE is feasible [13, 24–26].

The Method of Cardiac MRE

A conventional elastography experiment incorporates three major technical steps:

1. Mechanical tissue stimulation,
2. Measurement of the resulting deformation by MRI or ultrasound, and
3. Image analysis based on strain analysis or inversion of the wave equation [20].

Mechanical Tissue Stimulation

Various strategies using ultrasound or MRI for performing cardiac elastography have been pursued to assess alterations in myocardial elasticity during the cardiac cycle in a noninvasive way. Basically, three concepts of mechanical activation (i.e., application of stress) of the *in vivo* heart muscle for elastographic examinations have been used: a) intrinsic activation of the myocardium [13, 14, 27–29], b) internal stimulation of shear waves based on focused ultrasound impulses [15, 30–33], and c) externally induced shear waves from a time-harmonic vibration source [17, 34–36]. The wave sources used were loudspeakers attached to rigid pistons or pneumatic tubes for transferring acoustic energy onto the anterior chest wall. Time-harmonic shear waves in the low audible frequency range of 25 to 80 Hz can readily be introduced into the chest without significant attenuation. Moreover, the deposition of mechanical energy is negligible at low audio frequencies, since the continuous flux of shear wave energy through the tissue scales with the squared excitation frequency [37]. However, these advantages of low-frequency time-harmonic vibrations are bought at the cost of resolution since the thickness of the heart wall is smaller or on the same order as the length of the shear waves being measured. In such finite geometries, the propagation speed and the dispersion of shear waves depend on both intrinsic properties and the geometry of the medium [38].

Deformation Measurement

The resulting strain fields can be measured using ultrasound [39, 40] or MRI [41, 42]. Medical ultrasound is rather inexpensive, robust, and capable of strain estimation in real time. However, strain measurement is restricted to axial displacement. Phase-contrast MRI is known for quantification of blood flow and motion [43]. Phase-contrast MRI has the advantage of being intrinsically sensitive to motion in three dimensions, which is particularly useful for elastography. However, cardiac MRE still suffers from relatively long scanning times since wave images are acquired using *k*-space-segmented gradient echo sequences in synchrony with the electrocardiogram (ECG) over multiple heart beats [35, 44–46]. This periodicity of signal acquisition requires a

periodic mechanical stimulus matched to the repetition time of the MRI sequence. For this reason, the time-harmonic wave approach is most appealing in cardiac MRE since the synchronization of image acquisition and periodic mechanical stimulation cause steady states in both MR signal dynamics and mechanical tissue response [44, 47]. The mechanical steady state sustains a constant flux of wave energy through the heart, which is a prerequisite for analyzing the variation of shear wave amplitudes over the cardiac cycle.

Image Analysis (WI- and WAV-MRE)

Similar to other applications of MRE in the brain or liver, cardiac MRE is based on low-frequency time-harmonic vibrations. Unlike in bulky organs, shear waves in the heart are influenced by multiple nearby boundaries causing diffraction and waveguide effects. As a consequence, direct inversion of the time-harmonic wave equation for calculating quantitative stiffness maps is not feasible. Instead, one has to account for boundary conditions by modeling the myocardial wall by a plate [26, 48] or a thin shell [49, 50]. Algorithms for wave inversion (WI) in cardiac MRE remain the subject of investigation [50, 51]. A simplified analysis of time-harmonic waves accounts for shear wave amplitudes being altered due to the variation of the shear modulus in an unbounded, linear elastic and isotropic medium [45]. As a result, the relative variation in myocardial elasticity during the cardiac cycle is obtained. The advantage of the inversion-based approach is that it provides shear modulus values comparable to other MRE applications (in kPa). However, limitations arise from model assumptions such as wall thickness and singularities of the wave function at the poles of the sphere. In contrast, analyzing wave amplitudes does not require inversion and is thus less prone to time-varying boundary conditions in the heart. Although this approach implies many elastodynamic assumptions such as constant flux of shear wave energy through the heart, this so-called wave amplitude variation effect (WAV) was consistently observed in vivo by MRI and ultrasound [17, 34, 45, 52, 53, 54]. In current implementations, neither wave inversion-based cardiac MRE (WI-MRE) nor WAV-MRE accounts for anisotropic, hyperelastic, and poroelastic tissue properties. Diagrams on the principle of WI- and WAV-MRE are displayed in Fig. 1.

The technical key points of cardiac MRE can be summarized as follows: Time-harmonic waves between 25 Hz and 80 Hz are produced by distant wave sources and introduced into the chest by passive nonmagnetic transducers. Wave fields are acquired by gradient echo (GRE) sequences in synchrony with the periodicity of the mechanical vibration. Mechanical parameters are reconstructed by inversion of spherical waves within a thin shell or by analyzing the variation of shear wave amplitudes over the heartbeat. In the following, the two methods are referred to as wave inversion (WI) and wave amplitude variation (WAV) MRE.

Studies Performed Using Cardiac MR Elastography

WI-MRE [35, 49, 55, 56]

Phantom Experiments

In 2009, two phantom studies performed on a ventricular model of the heart [49, 55] showed a high correlation for MRE-derived data. Kolipaka and co-workers showed that, for cyclic pressure changes at 1 Hz ranging from 55 to 90 mmHg in a spherical silicon rubber phantom, MRE-based measures of shear stiffness highly correlated with values obtained using the pressure-volume model [49]. In a second study, changing heart rates ranging from 18–72 bpm were investigated. Stiffness estimates using a multiphase MRE-GRE sequence were stable as long as the fraction of the deformation period required for acquisition of a single image was not greater than 42 %. The instability of the multiphase-GRE-MRE sequence with higher view sharing might be attributed consecutively to the reduced temporal resolution and averaging [55].

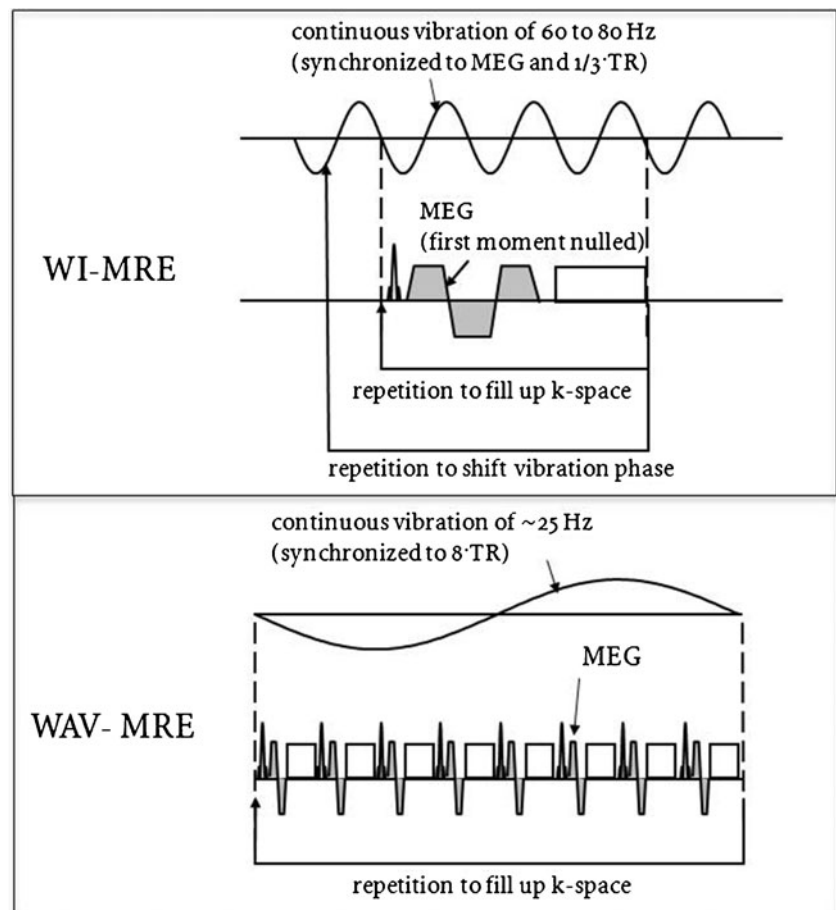
Animal Experiments

Following this work, the same study group investigated different driver configurations for MRE experiments in six pigs, and they compared MRE findings with LV pressure measurements. At 80 Hz excitation frequency (TR=12.5 msec), 20 phases of the cardiac cycle were reconstructed for different heart rates ranging between 63 and 100 bpm. A good correlation of LV pressure and MRE-derived stiffness values ($R^2=0.84$) was shown. The authors conclude that MRE has the potential for estimating effective myocardial stiffness throughout the cardiac cycle [35].

In 2011 and 2012, Kolipaka and co-workers published two studies, in which they investigated end-diastolic and end-systolic phases further. End-diastolic LV pressures were altered by different loading conditions (by dextran infusion). LV pressures were found to correlate linearly with MRE-derived effective stiffness measurements in four pigs (80 Hz excitation frequency, $R^2=0.73-0.9$) [57].

Investigations of end-systolic stiffness were performed in five animals [56]. Here, the authors showed, by finite element modeling (FEM), that phase gradient inversion could be performed on wall thicknesses of more than 15 mm. End-systolic effective stiffness was altered by epinephrine infusion so that heart frequency increased (85–188 bpm). In four animals, MRE-derived effective stiffness values showed a high correlation with heart rate, while a temporal resolution of 50–100 ms was achieved for the excitation frequency of 80 Hz (= TR*VPS; 12.5*4 to 8). In the fifth animal, no correlation ($R^2=0.1$) was found [56].

Fig. 1 Diagrams of WI-MRE (top) and WAV-MRE (bottom). The WI-MRE approach uses excitation frequencies of 60–80 Hz, resulting in a temporal resolution of 50–100 ms in the heart. With WAV-MRE a lower frequency shear waves (e.g., 23–25 Hz) is sampled at multiple (here 8) time points with a temporal resolution of TR. The effective temporal resolution is 41 ms ($8 \cdot TR$)



Feasibility Study in Normal Volunteers and Patients

In 2011, Kolipaka and co-workers presented a feasibility study conducted in healthy volunteers and patients with hypertrophic obstructive cardiomyopathy at the ISMRM meeting in Montreal [58]. With the technique previously tested in animals, ten cardiac phases were reconstructed in 18 healthy volunteers and two patients with hypertrophic obstructive cardiomyopathy (HOCM) in two short axes of the heart. The breath-hold technique—e.g., of about 14 seconds in end-expiration—showed that calculated mean effective stiffness in normal volunteers ranged between 3.5 and 7.9 kPa compared with stiffness values of 12 to 17.2 kPa in the two HOCM patients. An example of WI-MRE in a healthy volunteer is given in Fig. 2.

WAV-MRE

Correlation with Left Ventricular Pressure Measurement in Animals [52]

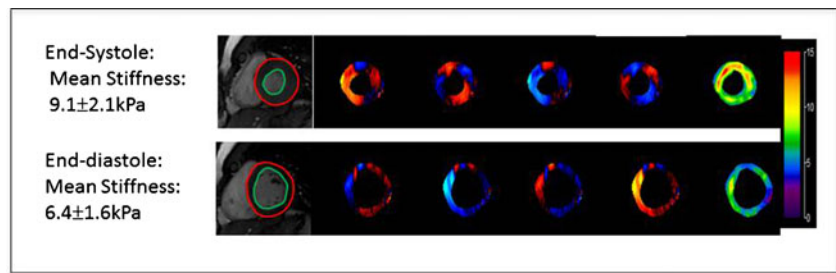
To estimate the sensitivity of cardiac MRE to left ventricular pressure, the time-resolved wave amplitudes measured by cardiac MRE were compared with invasive pressure

measurements taken by tip manometer in three minipigs. In all the animals, a time-dependent change in wave amplitudes in the left ventricle was noted. During systole lower shear wave amplitudes were observed, and during diastole higher wave amplitudes were measured. A good reciprocal correlation was shown between wave amplitudes and LV pressure ($R^2=0.76, 0.90, \text{ and } 0.96$). In contrast, no correlation was found between LV diameter and pressure measurements ($R^2 \leq 0.15$). Shear wave amplitudes changed before left ventricular diameter changes occurred. The measured ratios of wave amplitude changes between systole and diastole were 2.0–2.8, resulting in calculated pressure differences of 60–73 mmHg.

Findings in Healthy Volunteers [34]

In a study of eight healthy volunteers, cardiac MRE was performed using the change in induced shear wave amplitude as a relative measure of left ventricular pressure changes. As in the animal experiments, shear wave amplitude decreased during systole and increased during diastole. To compare these changes within and between participants, a model based on elastic wave theory and spherical shear stress was derived

Fig. 2 Example of WI-MRE showing derived mean stiffness values of 9.1 ± 2.1 kPa for end-systole and values of 6.4 ± 1.6 kPa for diastole in a short cardiac axis view. Image courtesy of A. Kolipaka, PhD, The Ohio State University



to deduce wave amplitudes and MRE derived pressure at two different time points. Subsequently, the systolic wave amplitudes measured were correlated with systolic blood pressure measured noninvasively at the left arm. The pressure changes calculated from MRE were plotted against the left ventricular volume changes. The area enclosed by this graph showed a mean pressure-volume work of 0.85 ± 0.11 joule/heartbeat in eight healthy volunteers, which correlated well with data from the literature [59, 60].

Diastolic Dysfunction and Cardiac Time Intervals [53•]

Times of isovolumetric contraction and relaxation and the resulting indices (e.g., Tei index) can be used to describe overall cardiac function [61, 62]. A study of 35 healthy volunteers and 11 patients with relaxation abnormalities

investigated MRE for determining isovolumetric cardiac time intervals. The magnitude of the complex signal was used to deduce morphological information, and magnitude combined with the phase of the complex signal was used to derive tension-relaxation information of systole and diastole. Wave amplitudes decreased during systolic contraction and increased during diastolic relaxation of the left ventricle. The changes in wave amplitude occurred well ahead of the morphological changes (Fig. 3). In healthy volunteers the mean cardiac time intervals of systole and diastole were 136 ± 36 ms and 75 ± 31 ms, respectively. In patients with diastolic dysfunction, the systolic cardiac time interval was 161 ± 45 ms, which is within the same range ($P=0.0053$). The diastolic time interval was 133 ± 57 ms and significantly prolonged ($P < 0.001$).

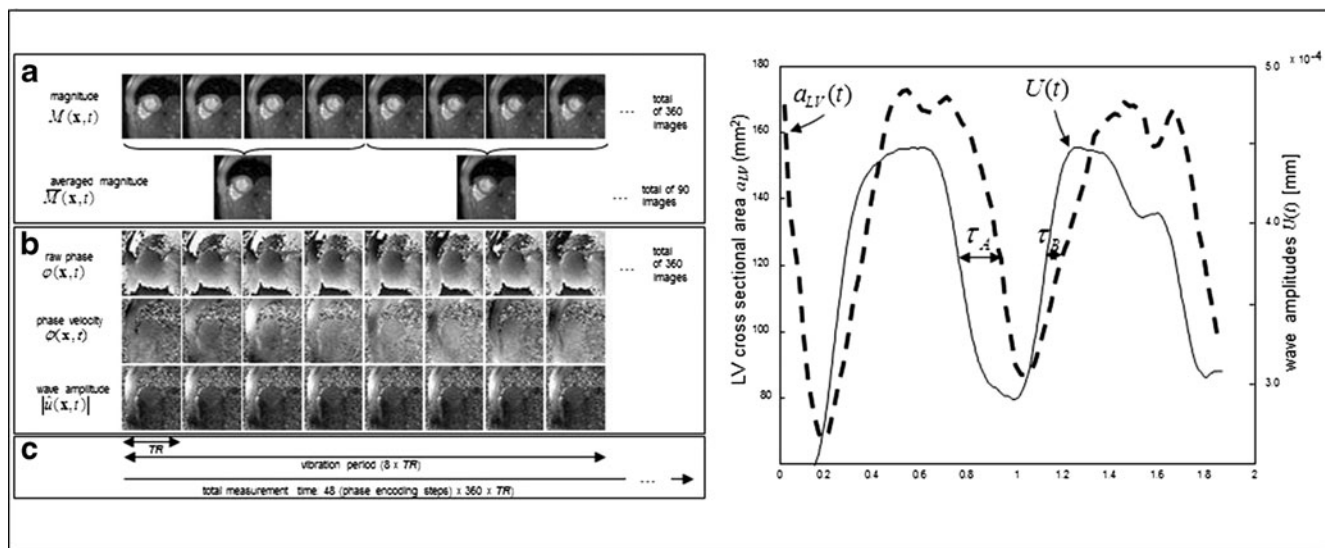


Fig. 3 Reproduced from Elgeti T et al., Elasticity-based determination of isovolumetric phases in the human heart, Journal of Cardiovascular Magnetic Resonance 2010,12:60; Figs. 2 and 3. On the left side the evaluation of the complex MRE signal for deducing morphological changes as well as variations in myocardial elasticity during the cardiac cycle is displayed. **a**: Ninety magnitude images $M(t)$ were generated from 360 magnitude images $M(t)$ by temporal averaging. The left ventricular cross-sectional area (α_{LV}) was segmented. **b**: Calculation of wave amplitudes $U(t)$ from 360 raw-phase images $\phi(x,t)$ involves three major

steps: i) unwrapping, ii) integration, and iii) Hilbert transform and display as magnitude $U(t)$. **c**: Illustrates the timing of image acquisition relative to a vibration period. The curves on the right side represent the temporal course of a healthy volunteer, outlining the changes in wave amplitude $U(t)$ (broken line) and the morphological changes in the left ventricular cross sectional area $\alpha_{LV}(t)$ (solid line). The changes in wave amplitude precede the morphological changes in left ventricular cross sectional area in systole (τ_A) and diastole (τ_B)

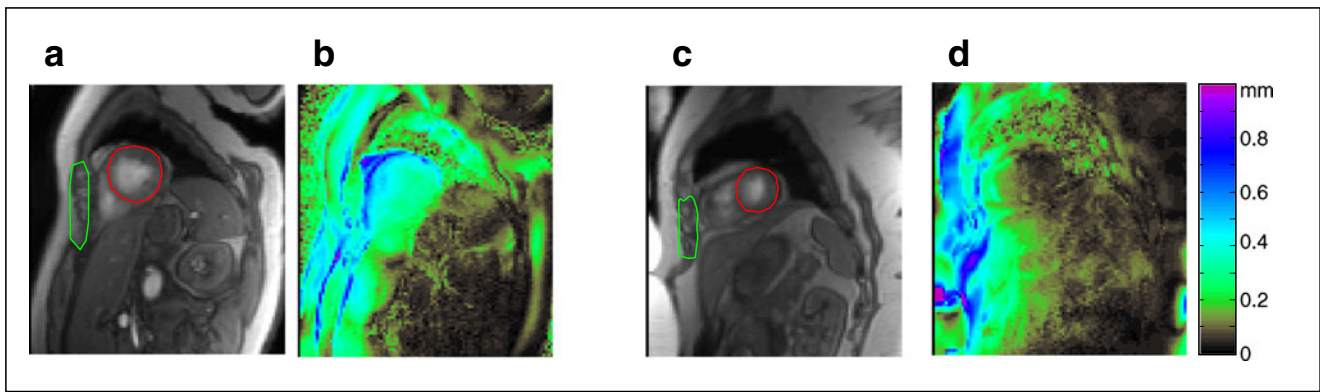


Fig. 4 Short cardiac axis of the heart with maps of a normal volunteer (**b**) and a patient with severe diastolic dysfunction (**d**). The corresponding magnitude reconstruction images from the complex MRE signal in the same slice orientation are given in (**a**) and (**c**). The red line outlines the

outer contour of the left ventricle during systole. The region of interest normalizing the induced shear waves anterior of the heart anterior of the heart is outlined in green

Diastolic Dysfunction [63]

As it is known that myocardial stiffness increases not only with myocardial disease [64] but also with age [65], a young and an old healthy group (mean age of 31.7 years versus 54.8 years) were compared to patients with diastolic dysfunction [63]. This was done by generating maps from the cardiac MRE experiments comprising all three Cartesian components. The maps were generated using the time-gradient operator for linear high-pass filtering and phase unwrapping, which was followed by temporal Fourier transformation for

separating the induced 24.3 Hz shear vibration from intrinsic cardiac motion and blood flow. As excitation amplitudes were adjusted to the individual subjects' comfort and as patients had a higher body mass index (BMI), the wave amplitudes measured in the left ventricle were normalized by wave amplitudes anterior to the heart, adjacent to the right ventricle. Two different maps of a healthy volunteer and a patient with diastolic dysfunction - are displayed in Fig. 4.

A feasibility study [63] followed by a study of 30 patients with different stages of diastolic dysfunction [66••] showed that normalized shear wave amplitudes

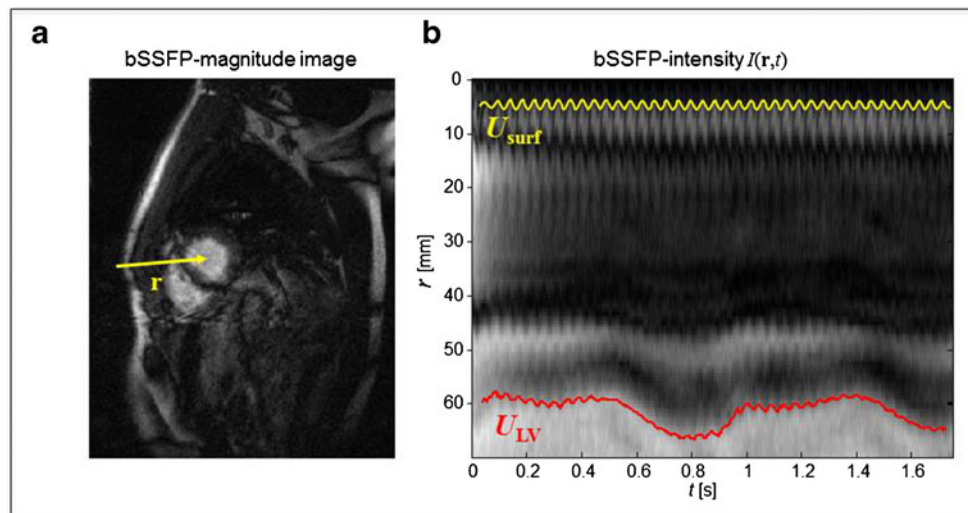


Fig. 5 Reproduced with kind permission of Wiley Periodicals Inc from Elgeti T et al. Magn Reson Med 67:919–924, 2012, Vibration-Synchronized Magnetic Resonance Imaging for the Detection of Myocardial Elasticity Changes; Fig. 2. **a**: Systolic short axis view of the heart using a magnitude image derived from a bSSFP acquisition to display cardiac

anatomy and the position of profile r . **b**: Profile r shown in (**a**) plotted over time using an M-mode like view. Vibrations due to the externally induced motion are very well visible in the chest wall, the anterior boundary of the right ventricle, and the interventricular septum

decrease with age. In patients, a significant decrease in normalized shear wave amplitudes is found. In this study a cutoff-value of 0.43 mm an AUROC value of 0.92 with 90 % sensitivity and 89.7 % specificity identified patients with diastolic dysfunction when compared to echocardiography as standard of reference.

Perspective: Vibration-Synchronized Magnetic Resonance Imaging (vsMRI) [36]

The strategy of WAV-MRE could readily be incorporated into a vibration synchronized morphological image acquisition sequence. In the approach of vibration-synchronized MRI (vsMRI) a cardiac triggered cine steady-state imaging sequence (bSSFP) synchronized with external harmonic motion displays oscillatory tissue deformations in magnitude images. The induced vibration (22.83 Hz) matched 12 repetition times (TR=3.65 ms) of the sequence. Data are acquired in 1.752 s per phase-encoding step (= 480 TR) so that more than one RR-interval is accomplished. During this time, a single phase-encoding step was performed for each image, while the chest was continuously vibrated by 40 cycles (i.e., 480/12) of the sinusoidal actuator motion. Imaging was performed with a matrix size of 256×192, a 400×300 mm field of view, a high in-plane resolution of 1.56 mm, and 5 mm slice thickness. By using parallel imaging acquisition techniques (GRAPPA, acceleration factor of 2), 108 phase-encoding steps were captured in about 7.5 min during controlled breathing.

Shear wave frequencies below 25 Hz penetrate the body without any major attenuation. Therefore, deflections approach the order of millimeters throughout the body. The externally induced motion is on the order of in-plane resolution of commonly used clinical MRI techniques. Oscillations therefore become visible in the morphological contrast of magnitude reconstructions. When a bSSFP sequence is used, the wave amplitude can best be measured at the endomyocardial-blood interface due to intrinsically high contrast between blood and myocardium. An image example showing analysis of signal intensity over time is given in Fig. 5. Unlike the conventional MRE techniques discussed earlier (i.e., both wave length-based and wave amplitude-based approaches), vsMRI requires no-phase contrast technique with motion encoding gradients for encoding the oscillatory motion. A conventional MRI sequence synchronized to the induced tissue vibrations serves to measure myocardial stiffness changes. As MEGs are not necessary, echo time and repetition time are shortened, and signal relaxation and susceptibility artifacts are reduced, while the temporal resolution of cine imaging is improved.

Limitations

Up to now, a limited number of researchers have applied cardiac MRE or have developed methods of their own for in vivo stiffness measurements in the heart indicating the strong experimental background of this promising technique. Therefore, the reported number of animals, volunteers, and patients investigated by cardiac MRE is still too small for the transfer of the method into the clinic. Further validation is urgently needed.

A major drawback of WI-MRE is the low temporal resolution of 50–100 ms. Although it is possible in principle to obtain quantitative values of shear stiffness, up to now only “effective” quantitative stiffness values have been reported for WI-MRE, since different influencing conditions such as intrathoracic pressure changes, pre- and afterload of the heart during the experiment are not known [35].

A major drawback of WAV-MRE is the need for normalization of wave amplitudes, yielding a relative measure of the time-varying shear modulus. As such, the shear waves measured by WAV-MRE can be regarded as a novel source of image contrast sensitive to mechanical tissue properties and intraventricular pressure rather than a measure for quantifying tissue stiffness.

Conclusion

Cardiac MRE is capable of providing mechanical image contrast sensitive to the shear-elastic properties of the myocardium. Since ventricular pressure arises from alterations in the shear modulus of the myocardial wall, MRE images can reveal the evolution of pressure during the cardiac cycle noninvasively. Therefore, cardiac MRE is considered particularly useful for the diagnosis of relaxation abnormalities characterized by an elevated pressure during the diastolic cardiac phase. To date, multiple validation studies performed on phantoms, animals, and healthy volunteers have been published as well as initial results obtained in patients with diastolic dysfunction. Larger groups of patients need to be investigated to determine the diagnostic power of cardiac MRE.

Compliance with Ethics Guidelines

Conflict of Interest Thomas Elgeti and Ingolf Sack declare that they have no conflict of interest.

Human and Animal Rights and Informed Consent This article does not contain any studies with human or animal subjects performed by any of the authors.

References

Papers of particular interest, published recently, have been highlighted as:

- Of importance
- Of major importance

1. Heidenreich PA, Albert NM, Allen LA, Blumke DA, Butler J, Fonarow GC, et al. Forecasting the impact of heart failure in the United States: a policy statement from the American Heart Association. *Circ Heart Fail*. 2013;6:606–19.
2. Roger VL, Go AS, Lloyd-Jones DM, Benjamin EJ, Berry JD, Borden WB, et al. Executive summary: heart disease and stroke statistics—2012 update: a report from the American Heart Association. *Circulation*. 2012;125:188–97.
3. Hunt SA, Abraham WT, Chin MH, Feldman AM, Francis GS, Ganiats TG, et al. 2009 Focused Update Incorporated Into the ACC/AHA 2005 Guidelines for the Diagnosis and Management of Heart Failure in Adults. *Circulation*. 2009;119:e391–479.
4. McMurray JJ, Adamopoulos S, Anker SD, Auricchio A, Böhm M, Dickstein K, et al. ESC Guidelines for the diagnosis and treatment of acute and chronic heart failure 2012 The Task Force for the Diagnosis and Treatment of Acute and Chronic Heart Failure 2012 of the European Society of Cardiology. Developed in collaboration with the Heart Failure Association (HFA) of the ESC. *European Heart Journal*. Eur Soc Cardiol. 2012;33:1787–847.
5. Bleumink GS, Knetsch AM, Sturkenboom MCJM, Straus SMJM, Hofman A, Deckers JW, et al. Quantifying the heart failure epidemic: prevalence, incidence rate, lifetime risk and prognosis of heart failure The Rotterdam Study. *Eur Heart J*. 2004;25:1614–9.
6. Kass DA. Assessment of diastolic dysfunction. Invasive modalities. *Cardiol Clin*. 2000;18:571–86.
7. Borlaug BA, Kass DA. Invasive hemodynamic assessment in heart failure. *Cardiol Clin*. 2011;29:269–80.
8. Hamon M, Lipiecki J, Carrié D, Burzotta F, Durel N, Coutance G, et al. Silent cerebral infarcts after cardiac catheterization: a randomized comparison of radial and femoral approaches. *Am Heart J*. 2012;164:449–54.e1.
9. Ordovas KG, Higgins CB. Delayed Contrast Enhancement on MR Images of Myocardium: Past, Present, Future. *Radiology*. Radiol Soc North Am Inc. 2011;261:358–74.
10. Coelho-Filho OR, Rickers C, Kwong RY, Jerosch-Herold M. MR myocardial perfusion imaging. *Radiology*. 2013;266:701–15.
11. Caudron J, Fares J, Bauer F, Dacher J-N. Evaluation of left ventricular diastolic function with cardiac MR imaging. *Radiographics*. 2011;31:239–59.
12. Jeung MY, Germain P, Croisille P, Ghannudi SE, Roy C, Gangi A. Myocardial Tagging with MR Imaging: Overview of Normal and Pathologic Findings. *Radiographics* [Internet]. 2012;32:1381–98. doi:10.1148/rg.325115098.
13. Konofagou EE, D'hooge J, Ophir J. Myocardial elastography—a feasibility study in vivo. *Ultrasound Med Biol*. 2002;28:475–82.
14. Kanai H. Propagation of spontaneously actuated pulsive vibration in human heart wall and in vivo viscoelasticity estimation. *IEEE Trans Ultrason Ferroelectr Freq Control*. 2005;52:1931–42.
15. Hsu SJ, Bouchard RR, Dumont DM, Wolf PD, Trahey GE. In vivo assessment of myocardial stiffness with acoustic radiation force impulse imaging. *Ultrasound Med Biol*. 2007;33:1706–19.
16. Urban MW, Pislaru C, Nenadic IZ, Kinnick RR, Greenleaf JF. Measurement of viscoelastic properties of in vivo swine myocardium using lamb wave dispersion ultrasound vibrometry (LDUV). *IEEE Trans Med Imaging*. 2013;32:247–61.
17. Tzschätzsch H, Elgeti T, Rettig K, Kargel C, Klaua R, Schultz M, et al. In Vivo Time Harmonic Elastography of the Human Heart. *Ultrasound in medicine & biology* [Internet]. Elsevier Ltd. 2012;38:214–22.
18. Wong VW-S, Chan HL-Y. Transient elastography. *J Gastroenterol Hepatol*. 2010;25:1726–31.
19. Vappou J. Magnetic resonance- and ultrasound imaging-based elasticity imaging methods: a review. *Crit Rev Biomed Eng*. 2012;40:121–34.
20. Glaser KJ, Manduca A, Ehman RL. Review of MR elastography applications and recent developments. *J Magn Reson Imaging*. 2012;36:757–74.
21. Wuerfel J, Paul F, Beierbach B, Hamhaber U, Klatt D, Papazoglou S, et al. MR-elastography reveals degradation of tissue integrity in multiple sclerosis. *Neuroimage*. 2010;49:2520–5.
22. Dokos S, Smail B, Young A. Shear properties of passive ventricular myocardium. *Am J Physiol Heart Circ Physiol*. 2002;2650–9.
23. van Heerebeek L, Borbély A, Niessen HWM, Bronzwaer JGF, van der Velden J, Stienen GJM, et al. Myocardial structure and function differ in systolic and diastolic heart failure. *Circulation*. 2006;113:1966–73.
24. Kanai H, Koiwa Y. Myocardial rapid velocity distribution. *Ultrasound Med Biol*. 2001;27:481–98.
25. Chen H, Varghese T, Rahko PS, Zagzebski JA. Ultrasound frame rate requirements for cardiac elastography: experimental and in vivo results. *Ultrasonics*. 2009;49:98–111.
26. Nenadic IZ, Urban MW, Mitchell SA, Greenleaf JF. Lamb wave dispersion ultrasound vibrometry (LDUV) method for quantifying mechanical properties of viscoelastic solids. *Phys Med Biol*. 2011;56:2245–64.
27. Kanai H. Propagation of vibration caused by electrical excitation in the normal human heart. *Ultrasound in medicine & biology*. 2009;35:936–48.
28. Luo J, Fujikura K, Homma S, Konofagou EE. Myocardial elastography at both high temporal and spatial resolution for the detection of infarcts. *Ultrasound Med Biol*. 2007;33:1206–23.
29. Pernot M, Fujikura K, Fung-Kee-Fung SD, Konofagou EE. ECG-gated, mechanical and electromechanical wave imaging of cardiovascular tissues in vivo. *Ultrasound Med Biol*. 2007;33:1075–85.
30. Bouchard RR, Hsu SJ, Palmeri ML, Rouze NC, Nightingale KR, Trahey GE. Acoustic radiation force-driven assessment of myocardial elasticity using the displacement ratio rate (DRR) method. *Ultrasound Med Biol*. 2011;37:1087–100.
31. Bouchard RR, Hsu SJ, Wolf PD, Trahey GE. In vivo cardiac, acoustic-radiation-force-driven, shear wave velocimetry. *Ultrason Imaging*. 2009;31:201–13.
32. Couade M, Pernot M, Messas E, Bel A, Ba M, Hagege A, et al. In vivo quantitative mapping of myocardial stiffening and transmural anisotropy during the cardiac cycle. *IEEE Trans Med Imaging*. 2011;30:295–305.
33. Pernot M, Couade M, Mateo P, Crozatier B, Fischmeister R, Tanter M. Real-time assessment of myocardial contractility using shear wave imaging. *J Am Coll Cardiol*. 2011;58:65–72.
34. Elgeti T, Rump J, Hamhaber U, Papazoglou S, Hamm B, Braun J, et al. Cardiac magnetic resonance elastography. Initial results. *Invest Radiol*. 2008;43:762–72.
35. Kolipaka A, Araoz PA, Mcgee KP, Manduca A, Ehman RL. Magnetic resonance elastography as a method for the assessment of effective myocardial stiffness throughout the cardiac cycle. *Magn Reson Med*. 2010;64:862–70.
36. Elgeti T, Tzschätzsch H, Hirsch S, Krefting D, Klatt D, Niendorf T, et al. Vibration-synchronized magnetic resonance imaging for the

- detection of myocardial elasticity changes. *Magn Reson Med.* 2012;67:919–24.
37. Achenbach JD. Wave propagation in elastic solids. Amsterdam: Elsevier; 1999.
 38. Graff KF. Wave Motion in Elastic Solids. Courier Dover Publications; 1991.
 39. Ophir J, Céspedes I, Ponnekanti H, Yazdi Y, Li X. Elastography: a quantitative method for imaging the elasticity of biological tissues. *Ultrasound Imaging.* 1991;13:111–34.
 40. Parker KJ, Huang SR, Musulin RA, Lerner RM. Tissue response to mechanical vibrations for “sonoelasticity imaging”. *Ultrasound Med Biol.* 1990;16:241–6.
 41. Plewes DB, Betty I, Urchuk SN, Soutar I. Visualizing tissue compliance with MR imaging. *J Magn Reson Imaging: JMRI.* 1995;5:733–8.
 42. Muthupillai R, Ehman RL. Magnetic resonance elastography. *Nat Med Nat Publ Group.* 1996;2:601–3.
 43. Moran PR, Moran RA, Karstaedt N. Verification and evaluation of internal flow and motion. True magnetic resonance imaging by the phase gradient modulation method. *Radiology. American Public Health Association;* 1985.
 44. Rump J, Klatt D, Braun J, Warmuth C, Sack I. Fractional encoding of harmonic motions in MR elastography. *Magn Reson Med.* 2007;57:388–95.
 45. Sack I, Rump J, Elgeti T, Samani A, Braun J. MR elastography of the human heart: noninvasive assessment of myocardial elasticity changes by shear wave amplitude variations. *Magn Reson Med.* 2009;61:668–77.
 46. Robert B, Sinkus R, Gennisson J-L, Fink M. Application of DENSE-MR-elastography to the human heart. *Magn Reson Med.* 2009;62:1155–63.
 47. Bieri O, Maderwald S, Ladd ME, Scheffler K. Balanced alternating steady-state elastography. *Magn Reson Med.* 2006;55:233–41.
 48. Nenadic IZ, Urban MW, Bernal M, Greenleaf JF. Phase velocities and attenuations of shear, Lamb, and Rayleigh waves in plate-like tissues submerged in a fluid (L). *J Acoust Soc Am.* 2011;130:3549–52.
 49. Kolipaka A, Mcgee KP, Araoz PA, Glaser KJ, Manduca A, Romano AJ, et al. MR elastography as a method for the assessment of myocardial stiffness: comparison with an established pressure-volume model in a left ventricular model of the heart. *Magn Reson Med.* 2009;62:135–40.
 50. Kolipaka A, Mcgee KP, Manduca A, Romano AJ, Glaser KJ, Araoz PA, et al. Magnetic resonance elastography: Inversions in bounded media. *Magn Reson Med.* 2009;62:1533–42.
 51. Manduca A, Oliphant TE, Dresner MA, Mahowald JL, Kruse SA, Amromin E, et al. Magnetic resonance elastography: non-invasive mapping of tissue elasticity. *Med Image Anal.* 2001;5:237–54.
 52. Elgeti T, Laule M, Kaufels N, Schnorr J, Hamm B, Samani A, et al. Cardiac MR elastography: comparison with left ventricular pressure measurement. *J Cardiovasc Magn Reson.* 2009;11:44.
 53. Elgeti T, Beling M, Hamm B, Braun J, Sack I. Elasticity-based determination of isovolumetric phases in the human heart. *J Cardiovasc Magn Reson.* 2010;12:60. *Study showing the potential of WAV-MRE in using magnitude and phase reconstruction of the complex MRE signal to determine elasticity-based cardiac time intervals.*
 54. Tzschätzsch H, Hättasch R, Knebel F, Klaua R, Schultz M, Jenderka K-V, et al. Original Contribution. *Ultrasound in medicine & biology.* Elsevier Ltd; 2013;1–7.
 55. Kolipaka A, Mcgee KP, Araoz PA, Glaser KJ, Manduca A, Ehman RL. Evaluation of a rapid, multiphase MRE sequence in a heart-simulating phantom. *Magn Reson Med.* 2009;62:691–8.
 56. Kolipaka A, Aggarwal SR, Mcgee KP, Anavekar N, Manduca A, Ehman RL, et al. Magnetic resonance elastography as a method to estimate myocardial contractility. *J Magn Reson Imaging.* 2012;36:120–7.
 57. Kolipaka A, Mcgee KP, Manduca A, Anavekar N, Ehman RL, Araoz PA. In vivo assessment of MR elastography-derived effective end-diastolic myocardial stiffness under different loading conditions. *J Magn Reson Imaging.* 2011;33:1224–8.
 58. Kolipaka A, McGee K, Aggarwal S, Anavekar N, Manduca A, Ehman R, et al. A feasibility study: MR elastography as a method to compare stiffness estimates in hypertrophic cardiomyopathy and in normal volunteers. Proceedings of the 19th Annual Meeting of the International Society of Magnetic Resonance in Medicine. Montreal; 2011. p. 274. *Very interesting feasibility study using the WI-MRE approach in healthy volunteers and two patients with HOCM, in whom this approach shows abnormally increased stiffness.*
 59. Alter P, Rupp H, Rominger MB, Klose KJ, Maisch B. A new methodological approach to assess cardiac work by pressure-volume and stress-length relations in patients with aortic valve stenosis and dilated cardiomyopathy. *Pflugers Arch.* 2008;455:627–36.
 60. Asanoi H, Kameyama T, Ishizaka S, Nozawa T, Inoue H. Energetically optimal left ventricular pressure for the failing human heart. *Circulation.* 1996;93:67–73.
 61. Tei C, Ling LH, Hodge DO, Bailey KR, Oh JK, Rodeheffer RJ, et al. New index of combined systolic and diastolic myocardial performance: a simple and reproducible measure of cardiac function—a study in normals and dilated cardiomyopathy. *J Cardiol.* 1995;26:357–66.
 62. Cui W, Roberson DA, Chen Z, Madronero LF, Cuneo BF. Systolic and diastolic time intervals measured from Doppler tissue imaging: normal values and Z-score tables, and effects of age, heart rate, and body surface area. *J Am Soc Echocardiogr Off Publ Am Soc Echocardiogr.* 2008;21:361–70.
 63. Elgeti T, Beling M, Hamm B, Braun J, Sack I. Cardiac Magnetic Resonance Elastography: Toward the Diagnosis of Abnormal Myocardial Relaxation. *Invest Radiol.* 2010;45:782–7.
 64. Rossi MA. Pathologic fibrosis and connective tissue matrix in left ventricular hypertrophy due to chronic arterial hypertension in humans. *J Hypertens.* 1998;16:1031–41.
 65. Gazoti Debessa CR, Mesiano Maifirino LB, Rodrigues de Souza R. Age related changes of the collagen network of the human heart. *Mech Ageing Dev.* 2001;122:1049–58.
 66. Elgeti T, Knebel F, Hättasch R, Hamm B, Braun J, Sack I. Shear wave amplitudes measured by cardiac magnetic resonance elastography for the diagnosis of diastolic dysfunction; *Radiology* 2013 in press. *Study investigating the diagnostic potential of WAV-MRE using normalized LV wave amplitudes. Data from 50 patients with two different age groups and three different groups of diastolic dysfunction are presented.*